

# Machine Learning-Based Sizing of a Renewable-Battery System for Grid-Connected Homes With Fast-Charging Electric Vehicle

Rahmat Khezri<sup>ID</sup>, Member, IEEE, Peyman Razmi<sup>ID</sup>, Amin Mahmoudi<sup>ID</sup>, Senior Member, IEEE, Ali Bidram<sup>ID</sup>, Senior Member, IEEE, and Mohammad Hassan Khooban<sup>ID</sup>, Senior Member, IEEE

**Abstract**—This paper develops a sizing model of solar photovoltaic (SPV), small wind turbine (SWT) and battery storage system (BSS) for a grid-connected home with a fast-charging plug-in electric vehicle (PEV). The home trades energy with the main grid under time-of-use tariffs for selling and purchasing electricity that affects the energy management. In this paper, a practical rule-based operation strategy is developed for the grid-connected home with fast-charging PEV that enables efficient and cheap energy management. The sizing problem is solved using a supervised machine learning algorithm, which is a feed forward neural network, by minimizing the cost of electricity. While the developed renewable-battery sizing model is general, it is examined using actual data of insolation, wind speed, temperature, load, grid constraints, as well as technical and economic data of BSS, SPV, SWT, and PEV in Australia. Uncertainty analysis is investigated based on ten scenarios of data for wind speed, temperature, load, insolation, and PEV. The effectiveness of the proposed model with fast-charging PEV is verified by comparing to slow charging and uncontrolled fast-charging models, as well as two other machine learning methods and a metaheuristic algorithm. It is found that the proposed model decreases the cost of electricity by 10.1% and 19.6% compared to slow charging and uncontrolled fast-charging models for the grid-connected home with PEV.

**Index Terms**—Battery, distributed renewable energy, electric vehicle, fast-charging, machine learning, optimal sizing.

Manuscript received 11 July 2022; revised 29 October 2022; accepted 30 November 2022. Date of publication 5 December 2022; date of current version 22 March 2023. Paper no. TSTE-00701-2022. (Corresponding author: Amin Mahmoudi.)

Rahmat Khezri is with the Department of Electrical Engineering, Chalmers University of Technology, 412 96 Gothenburg, Sweden (e-mail: rahmat.khezri@gmail.com).

Amin Mahmoudi is with the College of Science and Engineering, Flinders University, Bedford Park, SA 5042, Australia (e-mail: amaminmahmoudi@gmail.com).

Peyman Razmi is with the Department of Electrical and Computer Engineering, University of Porto, 4099-002 Porto, Portugal (e-mail: peyman.razmi65@gmail.com).

Ali Bidram is with the Department of Electrical and Computer Engineering, University of New Mexico, Albuquerque, TX 88003 USA (e-mail: ali-bidram@ieee.org).

Mohammad Hassan Khooban is with the Department of Electrical and Computer Engineering, Aarhus University, 8200 Aarhus, Denmark (e-mail: khooban@ieee.org).

Color versions of one or more figures in this article are available at <https://doi.org/10.1109/TSTE.2022.3227003>.

Digital Object Identifier 10.1109/TSTE.2022.3227003

## NOMENCLATURE

### A. Subscripts

<i>bs</i>	Battery energy storage system.
<i>dr</i>	Distributed renewable resources.
<i>i</i>	Component's type.
<i>h</i>	Home.
<i>pe</i>	Plug-in electric vehicle.
<i>sp</i>	Solar photovoltaic.
<i>sw</i>	Small wind turbine.
<i>u</i>	Imported from the grid
<i>vt</i>	Inverter
<i>z</i>	Exported to the grid.

### B. Superscripts

<i>at</i>	Actual.
<i>ch</i>	Charging state.
<i>ds</i>	Discharging state
<i>ip</i>	Input.
<i>max</i>	Maximum limitation
<i>min</i>	Minimum limitation
<i>ot</i>	Output.

### C. Parameters

<i>D</i>	Number of days in a year.
<i>D<sub>sp</sub></i>	Annual degradation of photovoltaic (%).
<i>D<sub>sw</sub></i>	Annual degradation of wind turbine (%).
<i>E<sub>bs</sub></i>	Rated energy of battery (kWh).
<i>E<sub>h</sub></i>	Total electricity demand of the home (MWh).
<i>FC<sub>charger</sub><sup>c</sup></i>	Capital cost for charger of electric vehicle (\$).
<i>FC<sub>i</sub><sup>c</sup></i>	Capital cost of each component (\$).
<i>FC<sub>i</sub><sup>m</sup></i>	Present maintenance cost of each component (\$).
<i>FC<sub>i</sub><sup>r</sup></i>	Present replacement cost of each component (\$).
<i>FC<sub>i</sub><sup>s</sup></i>	Present salvation cost of each component (\$).
<i>h<sub>c</sub></i>	Critical day hour (h).
<i>K<sub>i</sub><sup>m</sup></i>	Maintenance cost of each component (\$).
<i>K<sub>i</sub><sup>r</sup></i>	Replacement cost of each component (\$).
<i>s</i>	Interest rate (%).
<i>t</i>	Time (h).
<i>T</i>	Total time intervals in a year (h).
<i>v</i>	Project horizon (y).
<i>Y</i>	Year (y).

$\varphi_i$	Capital recovery factor for components cost.
$\eta_{bs}$	Efficiency of battery (%).
$\eta_{pe}$	Efficiency of electric vehicle's battery (%).
$\Delta t$	Time interval (h).

#### D. Variables

$AC_e$	Annual cost of electricity exchange between the home and grid (\$).
$ASP_e$	Annual supply of charge of electricity (\$).
$D_b$	Degradation of battery in each cycle (%).
$E$	Energy (kWh).
$E_{hp}$	Total electricity demand of home and plug-in electric vehicle (kWh).
$P$	Power at time $t$ (kW).
$P_m$	Dumped power (kW).
$R_i$	Replacement year of each component (y).
$TPC_i$	Total present cost of component $i$ (\$).
$SP_e$	Daily supply of charge (\$).
$O$	State of charge (%).
$W_i$	Remaining lifetime of each component at the end of project horizon (y).
$\alpha_i$	Number of each component.

## I. INTRODUCTION

WITH the development of plug-in electric vehicles (PEVs) in the premises of residential households, the demand is growing for fast-charging infrastructure at home [1]. The PEV with a fast charger brings convenience to the householders to charge their vehicles in a short time [2]. However, to reach a smart, cheap, and clean energy supply for the PEV and home, the household should be equipped with distributed renewable energy sources (DRESs) and battery storage system (BSS) [3]. Small wind turbines (SWTs) and rooftop solar photovoltaics (SPVs) are excellent options of DRESs for residential households.

Power utilities are moving toward advanced metering infrastructure that allows time-of-use (TOU) electricity tariffs for the customers. The TOU pricing tariff provides an economic driving force, for the customers, by making off-peak time more attractive for electricity usage [4]. Off-peak rates typically occur at night when the consumer sleeps. Therefore, charging a PEV at night results in a lower electricity cost. Especially if the consumers use fast charger, the PEV can be fully charged over the off-peak time quickly which is impossible by the conventional slow chargers. However, a grid-connected home with TOU tariff, PEV, DRESs, and BSS is a complex system in terms of economic analysis, energy management system (EMS), and sizing. Efficient EMS should be developed for such a home to achieve optimal sizing of BSS and DRES components with the minimum cost.

Several studies have investigated sizing problem of renewable-battery systems for residential sector. In [5], the optimal capacity of SPV and BSS was found for a grid-tied home without PEV. In [6], optimal sizing was investigated but EMS was not developed for the operation. Sizing of a standalone SPV-BSS system was investigated in [7]. A stochastic optimization framework by considering the real-time pricing (RTP) impact was considered in [8]. In [9], the effect of insolation uncertainty

was investigated on optimal sizing. The battery degradation effect was considered in sizing problem [10]. However, the impact of PEV on optimal sizing problem was not considered in all those studies.

Some studies were conducted on optimal sizing by considering PEVs. In [11], it was assumed that PEV are connected to the residential community while the capacity of SPV, SWT, and BSS was optimized. Planning of PEV charging station and distributed resources was investigated in [12], [13]. The effect of PEV's load modelling on the planning model was considered in [14]. The authors in [15], [16] considered bi-directional PEVs in smart grids. A new vehicle-to-grid (V2G) strategy was developed in [17]. However, the V2G strategies degrade the PEV's battery lifetime. Sizing of SPV and BSS for grid-connected homes with slow-charging PEVs was proposed in [18], [19]. However, none of the existing studies investigated sizing for grid-connected homes with fast-charging PEVs. This is a critical topic for sizing of renewable-battery system since the fast-charging model can be efficiently used to reduce the electricity cost.

To solve the optimal sizing problems, classic mathematical methods are extensively used. However, those methods cannot handle nonlinearities, complexity of the problem, and the battery lifetime which should be calculated based on the degradation [7]. Hence, metaheuristic methods like particle swarm optimization (PSO) [5], [6], [7], [8] and tabu search algorithm (TSA) [14] are used as alternatives for classic methods. Nonetheless, the metaheuristic methods have some essential drawbacks like high computational time and low exploration efficiency when confronted with large search spaces. To tackle these challenges, machine learning (ML) algorithms can be applied. The ML algorithms are model free, and hence they can handle complicated problems [20]. On the other hand, they will potentially learn in the training stage to handle different scenarios without difficulties [20]. Recently, the ML methods are successfully applied for power system operation problems in [20] and [21], but not for optimal sizing.

In addition to the above discussion, the existing studies did not develop EMS for the households with fast-charging PEVs. This is critical since installing fast charger at home would bring new opportunities for smart EMS design. The fast charger makes it possible to charge the PEV in a short time and hence it gives more flexibility to design EMS. In [18], [19], the EMSs were developed for the houses with slow-charging PEV under TOU and flat electricity tariffs. However, the current study develops a new practical EMS for the houses with fast-charging PEV that enables electricity cost reduction.

Table I presents a summary of the drawbacks in the existing studies based on the PEV, fast-charging, electricity tariff, EMS, uncertainty analysis, algorithm, and incorporation of real data. Incorporation of real data to achieve practical results was ignored by some studies. The effects of uncertainty parameters on the results were not investigated by several studies.

From a practical point of view, this study solves a timely problem of practicing engineering for an actual case study. The main novelty of this paper is to develop a practical EMS and sizing model of SPV, SWT, and BSS for grid-connected homes with fast-charging PEV. The majority of slow chargers

TABLE I  
SUMMARY OF DRAWBACKS OF THE EXISTING STUDIES

Ref.	PEV	FC	OA	ET	EMS	UA	RD
[5]	x	x	PSO	Flat	✓	✓	✓
[6]	x	x	PSO	TOU	x	x	✓
[7]	x	x	PSO	-	x	✓	✓
[8]	x	x	PSO	RTP	x	✓	x
[9]	x	x	Classic	TOU	x	✓	✓
[10]	x	x	SA	-	x	✓	x
[11]	✓	x	Classic	TOU	x	✓	x
[12]	✓	x	Classic	RTP	x	✓	x
[13]	✓	x	Classic	-	x	x	x
[14]	✓	x	TSA	RTP	✓	x	✓
[15]	✓	x	Classic	RTP	x	x	x
[16]	✓	x	Classic	-	x	✓	x
[17]	✓	x	Classic	RTP	✓	x	✓
[18]	✓	x	PSO	TOU	✓	✓	✓
[19]	✓	x	PSO	Flat	✓	✓	✓
This paper	✓	✓	ML	TOU	✓	✓	✓

FC: Fast charging; OA: Optimization algorithm; ET: Electricity tariff; UA: Uncertainty analysis; RD: Real data; TSA: Tabu search algorithm; PSO: Particle swarm optimization; SA: Simulation-based algorithm;

are rated at around 7 kW and will recharge a 100 kWh PEV in 12 hours by considering that SOC changes between 20% and 100%. However, the fast chargers are rated around 22 kW (for home application) and will recharge PEVs in less than 5 hours [22]. This shows the importance of the topic where the fast chargers can significantly reduce the charging time and accelerate the energy transition at home. To the best of authors' knowledge, this is the first study that considers a fast-charging PEV in grid-connected homes for sizing of a renewable-battery system. While the developed model is general, real measured data related to an Australian case study are incorporated to achieve practical results. The degradations of SPV, SWT, and BSS are incorporated into the developed model. The results of the fast-charging PEV are compared with those of slow-charging and immediate fast-charging models. The effects of fast charger power, maximum import/export powers from/to the grid, and the PEV's battery capacity on the optimization results are investigated. An uncertainty analysis is provided based on ten years stochastic data of load, wind, insolation, temperature, and PEV's data.

The main contributions of this study compared to previous works can be summarized as follows:

- A new optimal sizing model is developed for SPV, SWT, and BSS in a grid-connected home with fast-charging PEV. All practical parameters like grid constraint, real data, degradation of components, and salvation value are applied in the model.
- A practical rule-based operation strategy is proposed for a grid-connected home with fast-charging PEV. The operation strategy proposes a critical hour for charging the PEV by considering the fast-charging capability under TOU tariffs to reduce the electricity cost of the home.
- A supervised ML algorithm, which is a feed forward neural network to recognize patterns, is developed to solve the sizing problem. The supervised algorithm indicates promising results as compared to other ML and metaheuristic methods.

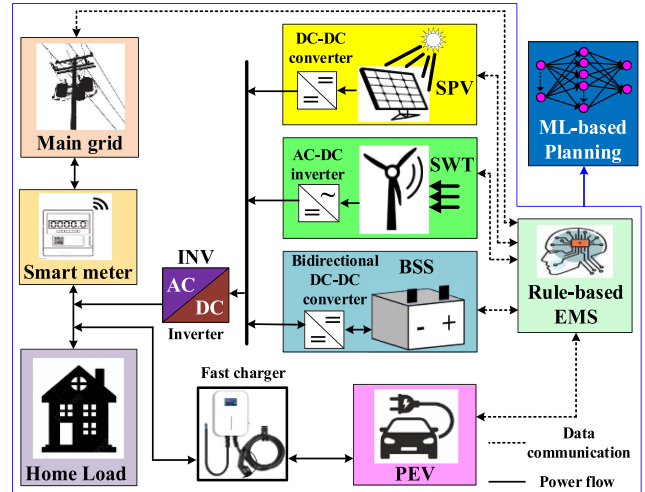


Fig. 1. System configuration of the studied grid-connected home.

## II. SYSTEM MODEL

The system configuration, operation strategy, as well as the components' models are presented in this section.

### A. System Configuration

Fig. 1 presents the single-line diagram of the system configuration for the grid-connected home with PEV, SPV, SWT, and BSS. The rooftop SPVs are extensively used by houses. Taking advantages of simple structure, reasonable cost, compact design, lower maintenance requirement, and portability, the SWTs are also suitable DRESs for residential areas [23]. There are both relevant literature [8] and actual engineering on application and installation of SWTs [24].

The SPV, SWT, and BSS are connected to a DC link. Then, a DC-AC inverter is used to connect the distributed resources to the load and grid. It is assumed that the BSS cannot be charged by the main grid. The PEV's operation in V2G or vehicle-to-home (V2H) modes are ignored in this study due to battery degradation effect [19].

### B. Operation Strategy

A new rule-based operation strategy is proposed for the grid-connected home in this study. The main features of rule-based operation strategy are lower computational requirement, ease of implementation, simple understanding, the ability to update the rules, and practicality [5].

Algorithm 1 presents the rule-based operation strategy for the grid-connected home with PEV, SPV, SWT, and BSS, under TOU electricity tariff. The proposed operation strategy considers electricity price, hour of the day, actual generation of SWT and SPV, and battery's energy state. It is notable that the grid limitations to manage the power flow and the battery limits on charging/discharging are also considered. This operation strategy is developed based on the fast-charging infrastructure of the home. For this aim, it is assumed that it is not necessary to charge the PEV by the main grid immediately after arrival.

This is because the fast charger gives the possibility to fully charge the PEV in a few hours. Hence, for the hours right after arrival, when the electricity price is high, the PEV can be only charged with SPV-SWT-BSS (if their generation is greater than the load). The charging process of the PEV is discussed in the next sub-section.

### C. Time of Use Model and Critical Hour

The TOU tariff divides the electricity price into two periods: off-peak (21-07) and peak (08-20). The electricity price at off-peak period is one-third of the peak period [9].

A critical hour ( $h_c$ ) is proposed in the operation strategy of this study to achieve lower cost of electricity. When the PEV arrives home and if the time is before the critical hour, it can be only charged with the DRESs and BSS. After the critical hour, the PEV can also be charged with the main grid. The  $h_c$  should be selected in a way that there would be enough time to completely charge the PEV by the main grid if there is not enough DRES generation and BSS energy before the PEV's departure. In this study, since the fast charger's power is 22 kW (for home application), the PEV's battery capacity is 100 kWh and the departure time is not before 5 am, the critical hour is selected as 12 pm. By selecting this critical hour, even in the worst condition, when the PEV arrives with an SOC of 20% and there is no generation from the SPV-SWT-BSS system, the main grid can fully charge the PEV with 22 kW at 5 hours (from 12 pm to 5 am).

### D. Distributed Renewable Sources Model

Mathematical models of SPV and SWT, given in [11], are used in this study. The output power of SPV and SWT is obtained using real measured data of wind speed, insolation, and temperature. Then, the actual power of DRESs is applied in the system model. This actual power can be calculated by:

$$P_{dr}^{at}(t) = \alpha_{sw} \cdot (1 - D_{sw})^v \cdot P_{sw}(t) + \alpha_{sp} \cdot (1 - D_{sp})^v \cdot P_{sp}(t) \quad (1)$$

where  $\alpha_{sw}$  and  $\alpha_{sp}$  are the number of SWT and SPV, respectively, to be optimized.  $P_{sw}$  and  $P_{sp}$  are the output power of SWT and SPV, respectively, at the rated capacity. The annual degradations of SPV and SWT are also considered in the proposed model.

### E. Battery and PEV's Charging Models

In each time interval, the charging/discharging power of BSS should not exceed an available power limit. The available input and output powers of battery for charging and discharging,  $P_{bs}^{ip}$  and  $P_{bs}^{ot}$ , respectively, can be given by:

$$P_{bs}^{ip}(t) = \min(\alpha_{bs} \cdot P_{bs}, (E_{bs}^{at}/\Delta t) \cdot (O_{bs}^{max} - O_{bs}(t))) \quad (2)$$

$$P_{bs}^{ot}(t) = \min(\alpha_{bs} \cdot P_{bs}, (E_{bs}^{at}/\Delta t) \cdot (O_{bs}(t) - O_{bs}^{min})) \quad (3)$$

where  $P_{bs}$  is the rated power of the BSS and  $\alpha_{bs}$  is the number of BSS to be optimized.

---

**Algorithm 1:** Ruled-Based Operation Strategy for the Grid-Connected Home With PEV, SPV, SWT, and BSS, Under TOU Electricity Pricing.

---

```

1: for t = 1: 8760 do
2:   if the actual power of DRESs ( $P_{dr}^{at}$ ) is higher than
    load
3:     and PEV's charging power then
4:       if the TOUz is off-peak price, then
5:         first supply the load and charge the PEV, then
charge the BSS, then export to the grid, dump the
extra power if any.
6:       else
7:         first supply the load and charge the PEV, then
export power to the grid, then charge the BSS,
dump the extra power if any.
8:       end if
9:     else
10:      if the TOUu is off-peak price, then
11:        if hour of the day is before  $h_c$ , then
12:          first supply the load and PEV with  $P_{dr}^{at}$ , then
import power from the grid to only supply the
load, then discharge the BSS.
13:        else
14:          first supply the load and PEV with  $P_{dr}^{at}$ , then
import power from grid to supply load and
PEV, then discharge the BSS.
15:        else
16:          if hour of the day is before  $h_c$ , then
17:            first supply the load and PEV with  $P_{dr}^{at}$ , then
discharge the BSS, then import power from
grid to only supply the load.
18:          else
19:            first supply the load and PEV with  $P_{dr}^{at}$ , then
discharge the BSS, import the remaining
power, if any, from the grid.
20:          end if
21:        end if
22:      end if
23:    end for

```

---

The SOC of BSS in each time interval is expressed by:

$$O_{bs}(t + \Delta t) = O_{bs}(t) + \frac{(P_{bs}^{ch}(t) \cdot \eta_{bs}^{ch} - P_{bs}^{ds}(t) / \eta_{bs}^{ds}) \cdot \Delta t}{E_{bs}^{at}} \quad (4)$$

The actual energy of the BSS ( $E_{bs}^{at}$ ) is calculated based on the rated energy of the battery ( $E_{bs}$ ) as follows:

$$E_{bs}^{at} = \alpha_{bs} \cdot E_{bs} \quad (5)$$

When the PEV is parked at home, its battery's SOC for each time interval is expressed by:

$$O_{pe}(t + \Delta t) = O_{pe}(t) + \frac{P_{pe}^{ch}(t) \cdot \eta_{pe}^{ch} \cdot \Delta t}{E_{pe}} \quad (6)$$

The available input power for charging of PEV is:

$$P_{pe}^{ip}(t) = \min(\alpha_{pe} \cdot P_{pe}, (E_{pe}/\Delta t) \cdot (O_{pe}^{max} - O_{pe}(t))) \quad (7)$$

Since the V2G and V2H operation modes of PEV are ignored in this study, its discharging power and thereupon its impact on the PEV's SOC are not incorporated.

#### F. Inverter Model

The nominal capacity of the inverter should be higher than the power that passes through it.

$$\eta_{vt} \cdot (P_{dr}^{at}(t) + P_{bs}^{ds}(t)) \leq \alpha_{vt} \cdot P_{vt} \quad (8)$$

where  $\eta_{vt}$  and  $P_{vt}$  are the efficiency and rated power of inverter.  $\alpha_{vt}$  is the number of inverters to be optimized.

It is notable that the extra power of DRESs is controlled by the inverter's control system using a voltage feedback loop [19]. This means that no physical dump load is applied.

### III. OPTIMAL SIZING MODEL

The sizing framework describes the objective function, feasibility constraints, and methodology to solve the problem.

#### A. Optimization Problem

An important economic indicator, known as cost of electricity (COE), is selected as the objective function. The optimization problem is formulated as follows:

$$f = \min_{\alpha_i} COE$$

$$COE = \frac{NPC_t + FC_{charger}^c}{E_{hp}} + \frac{AC_e}{E_{hp}} \quad (9)$$

Subject to:

$$\alpha_i^{min} \leq \alpha_i \leq \alpha_i^{max} \quad (10)$$

$$P_{dr}^{at}(t) + P_u(t) + P_{bs}^{ds}(t) - P_z(t) - P_{bs}^{ch}(t) - P_{pe}^{ch}(t) \\ = P_h(t) + P_m(t) \quad (11)$$

$$O_{bs}^{min} \leq O_{bs}(t) \leq O_{bs}^{max} \quad (12)$$

$$O_{pe}^{min} \leq O_{pe}(t) \leq O_{pe}^{max} \quad (13)$$

$$0 \leq P_{bs}^{ch}(t) \leq P_{bs}^{ip}(t) \quad (14)$$

$$0 \leq P_{bs}^{ds}(t) \leq P_{bs}^{ot}(t) \quad (15)$$

$$0 \leq P_{pe}^{ch}(t) \leq P_{pe}^{ip}(t) \quad (16)$$

$$0 \leq P_u(t) \leq P_u^{max} \quad (17)$$

$$0 \leq P_z(t) \leq P_z^{max} \quad (18)$$

$$O_{pe}(t = \text{departure}) \geq O_{pe}^{max} \quad (19)$$

Equation (9) is the objective function of the optimization problem. (10) to (19) represent the problem constraints of the optimization. The number of components is limited as shown in (10). The power balance between generation and consumption should be maintained by (11). The SOC of battery and PEV are

limited between minimum and maximum values as shown by (12) and (13), respectively. (14) and (15) represent the charging and discharging power constraints for the BSS, respectively. The charging power of PEV should not exceed the available input power (16). The imported and exported power from/to the grid should not exceed their maximum values as shown by (17) and (18), respectively. The SOC of PEV at the departure time should not be less than the maximum limit (19).

The total energy demand of the system ( $E_{hp}$ ) is obtained based on the annual home's load energy demand ( $E_h$ ) and the annual charging energy of the PEV ( $E_{pe}$ ) as follows:

$$E_{hp} = E_h + E_{pe} \quad (20)$$

$$E_h = \sum_{t=1}^T P_h(t), \quad E_{pe} = \sum_{t=1}^T P_{pe}^{ch}(t) \quad (21)$$

The COE is calculated based on the total net present costs of components ( $NPC_t$ ), capital cost of the charger for PEV ( $FC_{charger}^c$ ) and annual cost of electricity exchange between the home and grid ( $AC_e$ ) [5]. The  $NPC_t$  is calculated based on the total present cost of components as follows:

$$NPC_t = \varphi_i \cdot \sum_i (\alpha_i \cdot TPC_i) \quad (22)$$

The annual cost of electricity exchange between the home and grid ( $AC_e$ ) is given by:

$$AC_e = ASP_e + \sum_{t=1}^T U(t) \cdot P_u(t) \cdot \Delta t - \sum_{t=1}^T Z(t) \cdot P_z(t) \cdot \Delta t \quad (23)$$

The annual cost for supply of charge of electricity ( $ASP_e$ ) is calculated based on the daily supply of charge as follows:

$$ASP_e = \sum_{d=1}^D SP_e \quad (24)$$

The total present cost of each component ( $TPC_i$ ) can be calculated by:

$$TPC_i = FC_i^c + FC_i^r + FC_i^m - FC_i^s \quad (25)$$

The present capital cost of the components ( $FC_i^c$ ) is the investment cost at the beginning of the project. The present replacement cost of the components ( $FC_i^r$ ) can be given by:

$$FC_i^r = K_i^r \cdot \sum_{t=1}^{tY < v} \frac{1}{(1+s)^{tY}} \quad (26)$$

The present maintenance cost of the components ( $FC_i^m$ ) is calculated as follows:

$$FC_i^m = K_i^m \cdot \frac{(1+s)^v - 1}{s(1+s)^v} \quad (27)$$

The salvation cost is the value of the component at the end of project horizon, The present salvation cost of the components ( $FC_i^s$ ) can be expressed by:

$$FC_i^s = FC_i^c \cdot \frac{W_i}{R_i} \cdot \frac{1}{(1+s)^v} \quad (28)$$

The lifetime of SPV and SWT is predetermined. However, the lifetime of BSS should be estimated based on the operation of the system which affects the charging/discharging cycles of battery [25]. The Rainflow Cycle Counting Method (RCCM) is used to extract the cycles and their depth of discharge (DOD) value. In each full cycle ( $c$ ), the degradation of battery is calculated using an experimental model as follows [25]:

$$D_b(c) = \frac{\sigma_1}{\sigma_2 e^{-\sigma_3 D_oD(c)} + \sigma_4} \quad (29)$$

The values of parameters  $\sigma_1$  to  $\sigma_4$  are taken from [25]. The degradation of half cycles (counted by RCCM) is half of the full cycles. The degradations associated with all cycles during the annual operation are summed to obtain the total annual degradation. Once the total degradation becomes 20%, the battery lifetime reaches, and it should be replaced.

### B. Machine Learning Algorithm

Based on the described sizing model in (1)–(29), the objective function cannot be obtained in a closed form. Indeed, to calculate the BSS degradation via RCCM, future knowledge of SOC and DOD levels are needed. This issue barricades to connect the decision variables and objective function in a closed form. Hence, classical methods are unable to solve the problem.

In this study, a supervised machine learning algorithm, known as group method of data handling (GMDH), is used to solve the optimization model. This method is a feed forward neural network with supervised learning which allows the approximation of a function considering inputs and outputs. This method is broadly used in data mining, knowledge discovery, prediction, complex system modeling, pattern recognition, and optimization.

GMDH algorithms are characterized by inductive procedure that perform sorting-out of gradually complicated polynomial models and select the best solution by means of the external criterion. The general form of connection between inputs and output in a GMDH model can be expressed by a complicated polynomial series in the form of Volterra-Kolmogorov-Gabor polynomial, as below [26]:

$$\begin{aligned} y = & a_0 + \sum_{i=1}^n a_i x_i + \sum_{i=1}^n \sum_{j=1}^n a_{ij} x_i x_j \\ & + \sum_{i=1}^n \sum_{j=1}^n \sum_{k=1}^n a_{ijk} x_i x_j x_k + \dots \end{aligned} \quad (30)$$

where  $X(x_i x_j x_k, \dots)$  represents the vector of input variables,  $n$  is the limit of the variables' capacities,  $y$  represents the output value, and  $A(a_i a_j a_k, \dots)$  is the vector of coefficients which must be determined. In general, however, the proposed polynomial model in (30) is estimated in form of multiple binary quadratic equations in each layer as below [26]:

$$\bar{y} = a_0 + a_1 x_i + a_2 x_j + a_3 x_i x_j + a_4 x_i^2 + a_5 x_j^2 \quad (31)$$

All pairs of the neurons in each layer are calculated in form of (31), and then, the difference between the actual output  $y$  and the fitted value  $\bar{y}$  can be obtained. The coefficients of the model in

---

### Algorithm 2: The Developed Supervised Algorithm for Optimal Sizing of Components.

---

```

1: I. Training Process
2:   Historical data generation
3:   a) Consider a limit for number of SPV
4:   b) Consider a limit for number of SWT
5:   c) Consider a limit for number of BSS
6:   d) Select different scenarios for components
7:   for Number of SPV= 1 : max SPV do
8:     for Number of SWT= 1 : max SWT do
9:       for Number of BSS = 1: max BSS do
10:        Calculate COEs
11:         $x \leftarrow [\text{SPV } \text{SWT } \text{BSS } \text{INV}]$ 
12:        Save Decision Variables and COEs
13:         $X \leftarrow x$ 
14:         $Y \leftarrow \text{Costs}$ 
15:        Data  $\leftarrow [X \ Y]$ 
16:      end for
17:    end for
18:  end for
19: Train ML algorithm
20: II. Process to Find Optimal Solution
21: Getting initial decision variables and their COE0
22: for Iteration=1: Max Iteration (1000) do
23:   Getting randomly Decision Variables
24:   Prediction of COE
25:   if current COE < COE0, then
26:     COE0 $\leftarrow$  COE
27:   end if
28:   Optimal Value  $\leftarrow$  COE
29: end for
30: end for

```

---

each layer are calculated by minimizing the mean square error (MSE) of the difference between  $y$  and  $\bar{y}$  for all training data ( $N$ ):

$$\text{Min } \frac{1}{N} \sum_{i=1}^N (y_i - \bar{y}_i)^2 \quad (32)$$

For modeling the GMDH, the selection criterion and maximum model complexity are pre-selected. Then, the design process begins from the first layer. The number of layers and neurons in hidden layers of the model are determined automatically. All possible combinations of allowable inputs (all possible neurons) can be considered. Then, polynomial coefficients are determined using MSE as (32). Then, neurons that have better external criterion value (for testing data) are maintained, and others are removed. If the external criterion for layer's best neuron reaches minimum or surpasses the stopping criterion, network design is completed and the polynomial expression of the best neuron of the last layer is introduced as the mathematical prediction function; if not, the next layer will be generated, and this process continues [27], [28]. In this paper, it is considered that GMDH has 5 layers and there are 5 neurons in each layer. Algorithm 2 presents the developed supervised algorithm for sizing of components.

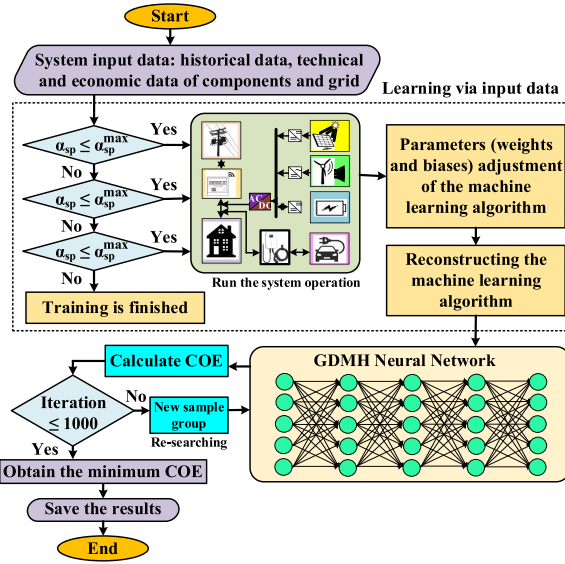


Fig. 2. Machine learning-based sizing algorithm to achieve the capacity of system components.

Fig. 2 indicates the ML-based sizing algorithm to achieve the capacity of SPV, SWT, BSS, and INV for the grid-connected home with fast-charging PEV. The algorithm starts with the input data containing the historical data, as well as the technical and economic data of components and grid. Then, the learning process is done based on the input data of the system. After the learning process, the initial results are generated by the GMDH. The re-sizing process is continued by the iterations. For each re-sizing process, the COE is calculated via the GMDH. Once all the iterations are done, the minimum COE is achieved, and the results are shown.

#### IV. SYSTEM UNDER STUDY

The developed sizing methodology is general and can be applied to any case studies. In this paper, however, it is examined on a real case study in Adelaide, Australia. A 3-phase grid-connected home is considered based on real data.

Fig. 3 indicates the real hourly measured load consumption data of the home, as well as the actual hourly measured wind speed and solar insolation of the location [5], [29]. The data is arranged for one year (8760 h).

Both import and export electricity rates are based on TOU tariffs. The import electricity price is 27.90 ¢/kWh for off-peak hours (21-07) and 42.90 ¢/kWh for peak hours (08-20) [9]. The export electricity price is assumed as one-third of the import price. In this paper, the costs are mentioned in Australian dollar.

Table II lists the input data of project, PEV, and components (i.e., SPV, SWT, IVT, and BSS) for the sizing problem. It is notable that a yearly degradation of 0.95% is considered for the SPV [7]. The annual degradation of SWT is considered as 1.6%. The system components data is taken from [25]. The round-trip efficiency of BSS and PEV's battery are considered as 92%. The costs are based on Australian dollar.

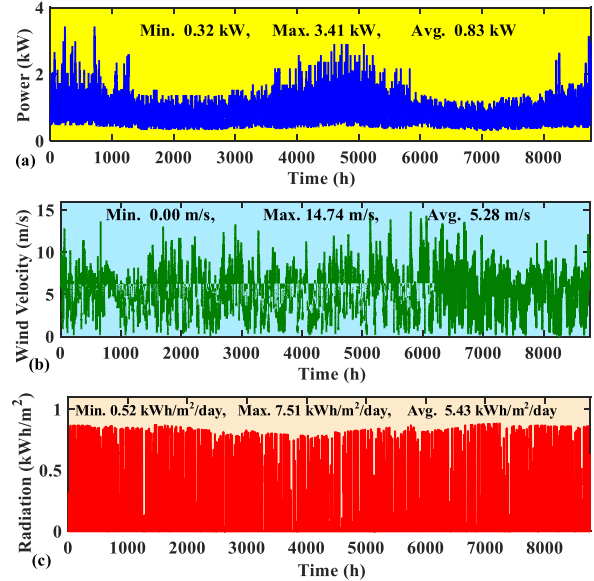


Fig. 3. Real hourly data for one year. (a) home electricity consumption, (b) wind velocity, and (c) solar radiation.

TABLE II  
INPUT DATA FOR THE OPTIMAL SIZING PROBLEM

<b>Project</b>	Project horizon = 10 years	
	Interest rate = 8%	Grid export constraint = 15 kW
	Escalation rate = 2%	Grid import constraint = 20 kW
<b>PEV</b>	Battery capacity = 100 kWh	Minimum SOC = 20% Maximum SOC = 95%
<b>SPV</b>	Unit size = 1 kW PV lifetime = 25 years	Capital cost = \$1,200 Maintenance cost= \$25/year
<b>SWT</b>	Unit size = 1 kW WT lifetime = 20 years	Capital cost = \$2,500 Maintenance cost= \$50/year
<b>IVT</b>	Unit size = 1 kW Inverter lifetime = 10 years	Capital cost = \$1,000 Inverter's efficiency= 95%
<b>BSS</b>	Unit size = 0.4 kW/ 1 kWh Minimum SOC = 10% Maximum SOC = 95%	Capital cost = \$500 Replacement cost = \$350 Maintenance cost = \$10/year

In South Australia, the 3-phase residential consumers are prohibited to export more than 15 kW power at any time to the distribution network [30]. The import power from the grid is limited to 20 kW.

The arrival SOC of PEV and its availability (departure and arrival times) data are produced by lognormal probability distribution function ( $PDF_{pe}$ ) as follows [19]:

$$PDF_{pe} (Q; \rho, \delta) = \frac{1}{Q \cdot \delta \cdot \sqrt{2\pi}} \cdot e^{-(ln X - \rho)^2 / 2\delta^2} \quad (33)$$

where  $Q$  shows the uncertainty parameter of the PEV to be set by the distribution function.  $\delta$  and  $\rho$  are the parameters for the standard deviation and mean value, respectively. The stochastic parameters for the distribution function of PEV are given in [19]. Fig. 4 shows the generated stochastic data for arrival SOC and the availability of PEV.

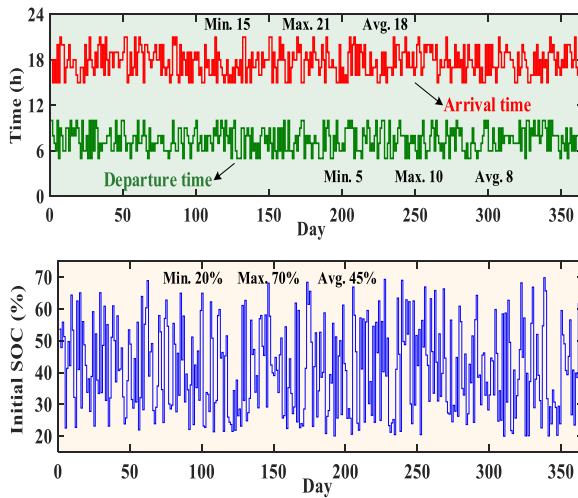


Fig. 4. Annual stochastic data for departure/arrival time and initial SOC of PEV at arrival.

TABLE III  
THE COE AND OPTIMIZED CAPACITY OF SYSTEM COMPONENTS

System	COE (¢/kWh)	SPV (kW)	SWT (kW)	BSS (kWh)	IVT (kW)
Fast-charging PEV (Proposed model)	26.77	20	5	2	17
Fast-charging PEV (Immediate charge)	33.27	19	2	3	14
Slow-charging PEV (Model in [18])	29.78	16	9	1	17

The price of the smart fast charger is considered as \$1200 that increases the charging power up to 22 kW compared to 7 kW of the smart slow charger with a price of \$800 [31]. The lifetime of the chargers is 10 years.

## V. RESULTS AND DISCUSSIONS

The optimization results (by comparison with other models), sensitivity analyses, and uncertainty analysis are provided in this section. The annual home's load energy demand is 7.25 MWh/year. Based on the initial SOC of PEV at arrival, the annual charging energy of the PEV is 17.39 MWh/year.

### A. Optimization Results

The proposed sizing model for grid-connected home with fast-charging PEV is compared with the same home with slow-charging PEV (7 kW charging power for PEV). It is also compared with an immediate fast-charging model. For this case, it is assumed that the charging of the PEV would start immediately after arrival until its battery is fully charged.

Table III indicates the COE of the models and the optimized capacities of SPV, SWT, BSS, and INV. As shown in the table, the proposed model results in the lowest COE (26.87 ¢/kWh) compared to the other models. The immediate model of the fast-charging PEV has the highest COE (33.25 ¢/kWh) because of the immediate charge of PEV after arriving when the TOU price is at peak time. The slow-charging model has a COE of 29.78 ¢/kWh which is lower than that of the immediate charge. In the

TABLE IV  
ANNUAL OPERATIONAL RESULTS OF THE STUDIED MODELS

System	TREG (MWh)	TIEG (MWh)	TEEG (MWh)	TDE (MWh)
Fast-charging PEV (Proposed model)	38.32	17.32	30.87	0.13
Fast-charging PEV (Immediate charge)	31.04	19.05	25.37	0.00
Slow-charging PEV (Model in [18])	40.41	15.72	31.31	0.21

TREG: Total renewable energy generation; TIEG: Total imported energy from the grid; TEEG: Total exported energy to the grid; TDE: Total dumped energy.

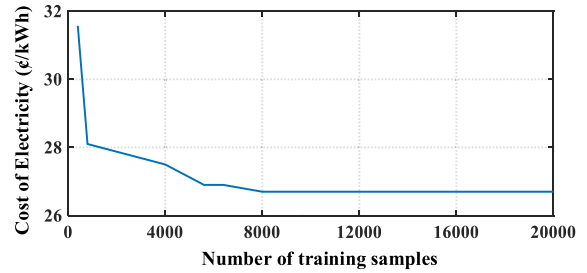


Fig. 5. Effect of the number of training samples for GMDH on the COE.

slow-charging model, the PEV is charged with 7 kW charge power and hence the charging period would be at both peak and off-peak times. It is seen that the proposed methodology for the fast charging decreases the COE by 3.01 ¢/kWh and 6.50 ¢/kWh compared to slow charging and immediate fast charging methods, respectively.

The sizing of the proposed fast-charging model results in 20 kW of SPV, 5 kW of SWT and 2 kWh of BSS as the capacity of the components. This system has the highest capacity of SPV, and it needs a 17-kW inverter. The capacity of SPV and SWT has decreased in the immediate model of the fast-charging PEV. However, the capacity of BSS is 1 kWh higher than that of the proposed model.

Table IV shows the annual operational results. The total renewable energy generation (TREG), total imported energy from the grid (TIEG), total exported energy to the grid (TEEG), and total dumped energy (TDE) are shown in the table. The TREG is the highest for the slow-charging system. As such, the TEEG and TDE are the highest for the slow-charging system. This is mainly because of the large capacity of the SWT in this system. Since the capacity of SPV and SWT are not high and the TREG is the lowest for the immediate model, it has no dumped energy. Around 80% of the TREG is exported to the main grid in the proposed model.

Further analyses on the proposed fast-charging model are provided in the next sub-sections.

### B. Analysis of Training Process of GMDH

In this study, the optimization is repeated by different number of training samples to ensure that the minimum COE is obtained. Fig. 5 shows the effect of number of training sample of GMDH on the COE. In this analysis, the number of samples are changed between 500 and 20000, for the training of GMDH. The optimization is repeated by steps of 500 samples in the considered

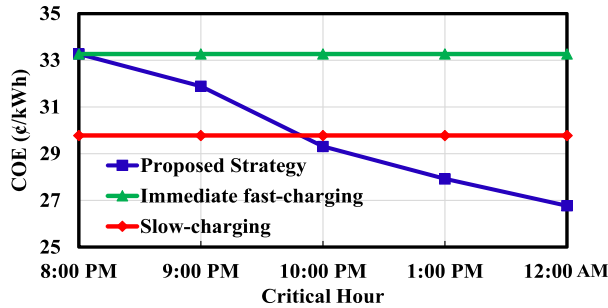


Fig. 6. Effect of critical hour on the COE of the optimized system by the proposed strategy and the other two strategies.

interval. As shown, the GMDH method has low accuracy for less than 8000 samples in the training process. As the number of samples decreases from 8000, the optimization accuracy is deteriorated and higher value of COE is obtained. On the other hand, for more than 8000 samples, the obtained or minimum COE (26.77 €/kWh) by the GMDH algorithm is not changed. Hence, we selected 8000 of samples as a reliable number to train the GMDH algorithm for the optimal sizing problem.

### C. Critical Hour Analysis

An analysis is provided on the proposed critical hour for charging of the PEV. Fig. 6 shows the effect of critical hour on the COE of the optimized system by the proposed strategy and the other two strategies. As depicted, the COE of slow-charging and immediate fast-charging strategies is not affected by changing the critical hour. However, as the critical hour decreases from 12 pm to 8 pm, the COE of the proposed fast-charging strategy increases. If the critical hour is selected as 8 pm, then the COE of the proposed strategy would be the same as that of the immediate charge strategy. This is due to the peak time of the TOU tariff which starts from 9 pm. Critical hours after 12 pm are not possible since there would not be enough time to fully charge the PEV's battery.

### D. Sensitivity Analysis

Sensitivity analyses are provided to investigate the effects of the PEV's charger power, maximum import/export power from/to the grid, SPV's capacity, and the PEV's battery capacity on the optimization results of the proposed fast-charging model.

The PEVs have different battery capacities in the market that may affect the COE of the home. Fig. 7 demonstrates the effects of the PEV's battery capacity on the COE and optimized capacity of the components. The COE increases from 26.3 €/kWh to 27.02 €/kWh when the PEV's battery capacity increases from 60 kWh to 160 kWh. The components have lower capacities for the 60 kWh and 80 kWh PEV's battery capacities. The capacity of SWT has increased to 8 kW when the PEV's battery capacity is 160 kWh.

The PEV's charger power could be installed in different powers to support the PEV's charging. For example, in this paper, the charger for fast-charging supported 22 kW power; however, the slow-charging supported 7 kW power. Hence, it is important to investigate a range of charger power for PEV's

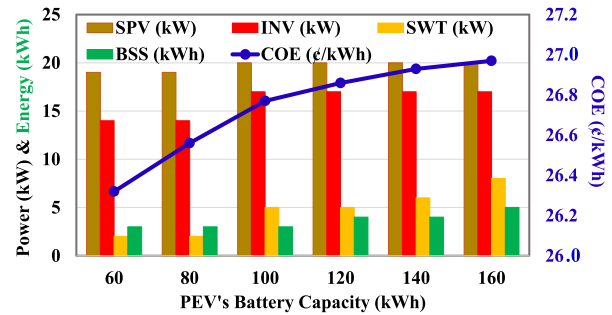


Fig. 7. Effects of the PEV's battery capacity on the COE and optimized capacity of the components.

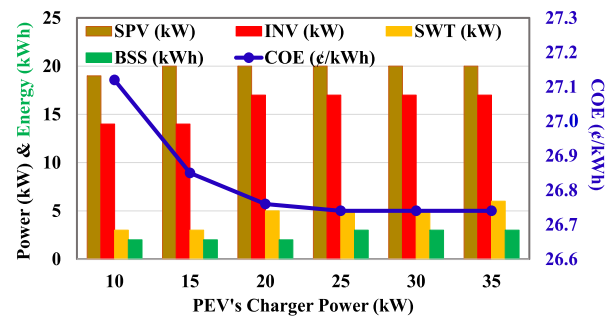


Fig. 8. Effects of the PEV's charger power on the COE and optimized capacity of the components.

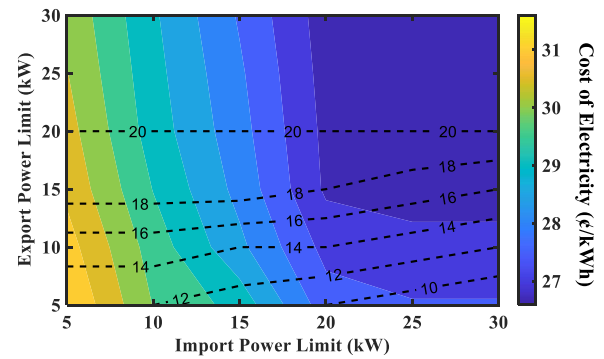


Fig. 9. Effects of export and import power limits on the COE and SPV capacity of the grid-connected home with fast-charging PEV. (Dashed line shows the capacity of SPV in kW).

charging in the premises of the grid-connected home. Fig. 8 illustrates the impacts of the PEV's charger power on the COE and optimized capacity of the components. As shown in the figure, the COE decreases when the charger power increases. However, the charger powers greater than 25 kW have no impact in the COE. The capacity of SPV remains constant (20 kW) for all PEV's charge powers. However, the capacities of SWT and BSS increase when the charger's power is higher than 20 kW.

The limitations on import and export powers from/to the grid may impact the optimal sizing results. Fig. 9 demonstrates the effects of export and import power limits on the COE of the grid-connected home with fast-charging PEV. Since the capacity of SPV has significantly changed in this scenario, the dashed line shows the capacity of SPV in kW in the figure. It is shown that

TABLE V  
EFFECTS OF SPV'S CAPACITY ON THE COE OF THE SYSTEM

Capacity of SPV (kW)										
2	4	6	8	10	12	14	16	18	20	
COE (€/kWh)	29.27	29.06	28.85	28.59	28.33	28.02	27.70	27.31	26.98	26.77

TABLE VI  
AVERAGE WIND SPEED, AVERAGE DAILY INSOLATION, AVERAGE TEMPERATURE, AND AVERAGE ANNUAL DAILY LOAD IN THE SCENARIOS FOR UNCERTAINTY ANALYSIS [18] AND [19]

Par.	S1	S2	S3	S4	S5	S6	S7	S8	S9	S10
AWS	5.3	4.9	5.1	5.4	4.8	4.9	5.0	4.7	5.2	5.3
ADI	5.4	5.6	5.1	5.0	5.2	5.1	5.7	5.2	5.3	5.4
AT	16.7	17.4	16.5	16.6	16.8	16.4	17.2	17.1	17.5	17.8
AADL	19.9	19.2	20.4	18.9	19.5	19.8	20.2	19.1	19.6	19.7

Par: Parameter; S: Scenario; AWS: Average wind speed (m/s); ADI: Average daily insolation (kWh/m<sup>2</sup>/day); AT: Average temperature (°C); AADL: Average annual daily load (kWh/day).

as the export power limit to the grid decreases, the capacity of the SPV decreases. For example, when the export power limit decreases from 20 kW to 10 kW, the SPV's capacity decreases from 20 kW to 15 kW. However, the export power limit has lower impact on the COE compared to the import power limit. The COE increases when the import power limit falls because the power deficit should be compensated by the SPV-SWT-BSS system.

The effect of SPV's capacity on the COE is presented for different capacities of the SPV from 2 kW to 20 kW. The optimization has been done separately for each capacity and the results are shown in Table V. It is shown that the COE of the system increases from 26.77 €/kWh to 29.27 €/kWh by reducing the SPV's capacity from 20 kW to 2 kW.

### E. Uncertainties Impacts

The impact of uncertainties of wind speed, solar insolation, ambient temperature, PEV's data, and electricity consumption on the optimal capacities is investigated for 10 different scenarios. The uncertainty scenarios are generated based on actual data, as well as uncertainty parameters and stochastic functions. For this purpose, the actual wind speed, insolation, and temperature data in Adelaide, Australia, over 10 years (2009-2018) is utilized [29]. The PEV's uncertainties for the availability (departure and arrival times) and level of SOC at arrival time are separately generated by (33) for each scenario. The electricity consumptions of the above 10 scenarios (or years) are obtained by adding uncertainty parameters to the available actual data as follows:

$$P_h^{scenarios}(t) = P_h(t) + P_h(t) \cdot \mu \cdot \gamma(t) \quad (34)$$

where  $P_h^{scenarios}$  is the generated electricity consumption uncertainty for each scenario (year),  $\gamma$  is a function to generate random numbers between -1 and +1, and  $\mu$  is a deviation factor with a value from 10% to 50% for each scenario.

Table VI lists the average annual wind speed, average daily insolation, average temperature, and average annual daily load in the uncertainty scenarios. The sizing model is run for each scenario, separately, and the results are analysed.

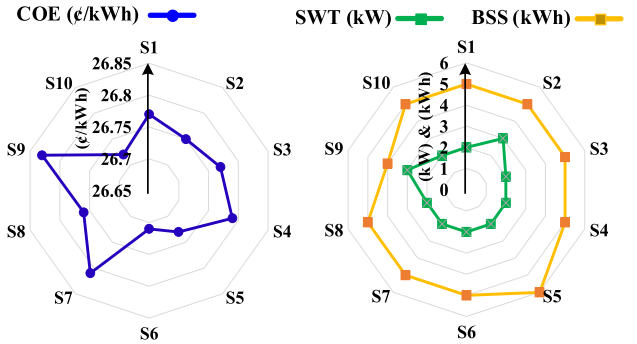


Fig. 10. The optimized COE, SWT capacity, and BSS capacity for the grid-connected home with fast-charging PEV for uncertainty scenarios 1–10.

TABLE VII  
COMPARISON OF THE ALGORITHMS FOR THE OBTAINED COE AND OPTIMIZED CAPACITY OF COMPONENTS

Method	COE (€/kWh)	SPV (kW)	SWT (kW)	BSS (kWh)	IVT (kW)
GMDH (This study)	26.77	20	5	2	17
MLP [32]	26.89	19	9	4	16
Bagging [33]	26.86	20	7	3	17
PSO [8]	26.84	20	6	3	17

Fig. 10 shows the COE, SWT capacity, and BSS capacity for the grid-connected home with fast-charging PEV for uncertainty scenarios 1–10. It is notable that the capacities of SPV and INV are not shown in the figure since their capacities remained constant in 20 kW and 17 kW, respectively, for all scenarios of uncertainty analysis. As shown in the figure, the COE changes between 26.65 €/kWh and 26.85 €/kWh in the scenarios. Hence, there is not significant change in the COE of the home, and this confirms the validity of the optimal results for COE based on 10 scenarios of uncertainty analysis. The capacities of the SWT and BSS are found as 5 kW and 2 kWh in eight scenarios. It can be confirmed that the capacity of the components is reasonable against the uncertainties for a grid-connected home with fast-charging PEV.

### F. Comparison With Other Algorithms

The results of the proposed GMDH method are compared with two other machine learning algorithms and a benchmark metaheuristic algorithm for sizing of the grid-connected home with fast-charging PEV. The ML algorithms are known as multi-layer perceptron (MLP) approach [32] and bagging method [33]. The benchmark metaheuristic algorithm is known as particle swarm optimization (PSO) which is broadly used for optimal sizing problems [5], [6], [7], [8]. Table VII lists and compares the results of the methods for COE and capacity of SPV, SWT, BSS, and INV. As indicated in the table, the GMDH method achieves the lowest COE compared to other methods. The COE of the bagging method is 0.03 €/kWh lower than that of the MLP method. While the COE obtained by the PSO algorithm is around 0.02 €/kWh lower than the bagging method, it is yet 0.07 €/kWh higher than that of the GMDH method. All bagging, MLP, and PSO methods result in higher capacity for SWT, and

TABLE VIII  
COMPUTATIONAL TIME OF ALGORITHMS TO SOLVE THE OPTIMAL  
SIZING PROBLEM

Method	GMDH	MLP	Bagging	PSO
Computational time	5.46 s	23.26 s	16.33 s	124.21 s

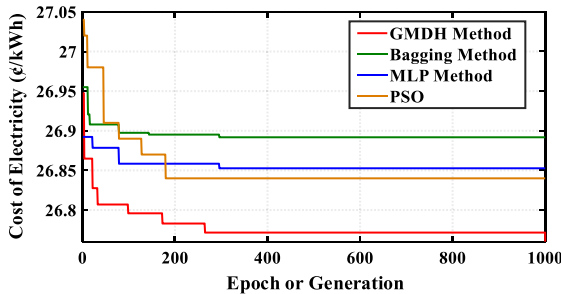


Fig. 11. Convergence pattern of the metaheuristic and machine learning algorithms for optimal sizing of the grid-connected home with fast-charging PEV.

BSS compared to the GMDH method. The highest capacity of SWT is obtained by the MLP algorithm as 9 kW. The INV's capacity is 17 kW for the GMDH, bagging, and PSO methods. Table VIII shows the computational times of GMDH, bagging method, MLP, and PSO algorithm. The GMDH method has the lowest computational time (5.46 s) as compared to other methods. The computational time of the PSO algorithm is much higher than the ML algorithms.

Fig. 11 shows the convergence pattern of ML algorithms for sizing of the grid-connected home with fast-charging PEV. The ML methods are run for 1000 epochs while the PSO algorithm is run for 1000 generation. For the machine learning algorithms, an epoch is a measure of the number of times that all the training vectors are used to update the weights. As demonstrated, the GMDH method is converged to the minimum COE in 261 epochs. However, the MLP and bagging methods are converged to their minimum COEs after 296 and 295 epochs, respectively. From the convergence viewpoint, the PSO works better than the ML algorithms by converging after 181 generations.

## VI. CONCLUSION AND FUTURE WORK

This study investigated optimal sizing of a renewable-battery system for grid-connected homes with a fast-charging PEV. A practical rule-based operation strategy was developed where a critical hour was proposed to control the PEV's charging by the SPV-SWT-BSS or the grid. The optimization problem was solved using a machine learning algorithm for a real case study in Australia. The proposed fast-charging model achieved 20 kW, 5 kW, 2 kWh, and 17 kW as the optimal capacities of SPV, SWT, BSS, and IVT. The proposed model reduced the COE by 10.1% and 19.6% compared to slow charging and uncontrolled fast-charging models for the grid-connected homes with PEV. The uncertainty analysis confirmed the validity of the optimal results based on 10 scenarios of stochastic data for load, PEV, wind, insolation, and temperature. It was shown that increasing the critical hour from 8 pm to 12 am would significantly decrease

the COE. Moreover, increasing the PEV's charger power to more than 25 kW had no effect on the COE.

The study can be further extended in future to investigate the effects of vehicle-to-grid (V2G) and vehicle-to-home (V2H) on the sizing problem. It is important to see if the V2G and V2H technologies decrease or increase the COE. The application of other new machine learning algorithms, to solve the optimal sizing problem, may represent another excellent direction for future works.

## REFERENCES

- [1] A. Amer, A. Azab, M. A. Azzouz, and A. S. A. Awad, "A stochastic program for siting and sizing fast charging stations and small wind turbines in urban areas," *IEEE Trans. Sustain. Energy*, vol. 12, no. 2, pp. 1217–1228, Apr. 2021.
- [2] Y. Zhang, Y. Zhou, C. Jiang, Y. Wang, R. Zhang, and G. Chen, "Plug-in electric vehicle charging with multiple charging options: A systematic analysis of service providers' pricing strategies," *IEEE Trans. Smart Grid*, vol. 12, no. 1, pp. 524–537, Jan. 2021.
- [3] F. Hafiz, A. R. de Queiroz, and I. Husain, "Coordinated control of PEV and PV-based storages in residential systems under generation and load uncertainties," *IEEE Trans. Ind. Appl.*, vol. 55, no. 6, pp. 5524–5532, Nov./Dec. 2019.
- [4] R. Khezri, A. Mahmoudi, and H. Aki, "Optimal planning of solar photovoltaic and battery storage systems for grid-connected residential sector: Review, challenges and new perspectives," *Renewable Sustain. Energy Rev.*, vol. 153, Jan. 2022, Art. no. 111763.
- [5] R. Khezri, A. Mahmoudi, and M. H. Haque, "Optimal capacity of solar PV and battery storage for Australian grid-connected households," *IEEE Trans. Ind. Appl.*, vol. 56, no. 5, pp. 5319–5329, Sept./Oct. 2020.
- [6] S. Bandyopadhyay, G. R. C. Mouli, Z. Qin, L. R. Elizondo, and P. Bauer, "Techno-economical model based optimal sizing of PV-battery systems for microgrids," *IEEE Trans. Sustain. Energy*, vol. 11, no. 3, pp. 1657–1668, Jul. 2020.
- [7] B. Mohandes, S. Acharya, M. S. E. Moursi, A. S. Al-Sumaiti, H. Doukas, and S. Sgouridis, "Optimal design of an islanded microgrid with load shifting mechanism between electrical and thermal energy storage systems," *IEEE Trans. Power Syst.*, vol. 35, no. 4, pp. 2642–2657, Jul. 2020.
- [8] S. Kahrobaee, S. Asgarpoor, and W. Qiao, "Optimum sizing of distributed generation and storage capacity in smart households," *IEEE Trans. Smart Grid*, vol. 4, no. 4, pp. 1791–1801, Dec. 2013.
- [9] M. Aghamohamadi, A. Mahmoudi, and M. H. Haque, "Two-stage robust sizing and operation co-optimization for residential PV-battery systems considering the uncertainty of PV generation and load," *IEEE Trans. Ind. Inform.*, vol. 17, no. 2, pp. 1005–1017, Feb. 2021.
- [10] T. Sayfutdinov et al., "Degradation and operation-aware framework for the optimal siting, sizing, and technology selection of battery storage," *IEEE Trans. Sustain. Energy*, vol. 11, no. 4, pp. 2130–2140, Oct. 2020.
- [11] R. Atia and N. Yamada, "Sizing and analysis of renewable energy and battery systems in residential microgrids," *IEEE Trans. Smart Grid*, vol. 7, no. 3, pp. 1204–1213, May 2016.
- [12] B. Zeng, H. Dong, R. Sioshansi, F. Xu, and M. Zeng, "Bilevel robust optimization of electric vehicle charging stations with distributed energy resources," *IEEE Trans. Ind. Appl.*, vol. 56, no. 5, pp. 5836–5847, Sep./Oct. 2020.
- [13] M. F. Shaaban, S. Mohamed, M. Ismail, K. A. Qaraqe, and E. Serpedin, "Joint planning of smart EV charging stations and DGs in eco-friendly remote hybrid microgrids," *IEEE Trans. Smart Grid*, vol. 10, no. 5, pp. 5819–5830, Sep. 2019.
- [14] A. Ahmadian, M. Sedghi, and M. Aliakbar-Golkar, "Fuzzy load modeling of plug-in electric vehicles for optimal storage and DG planning in active distribution network," *IEEE Trans. Veh. Technol.*, vol. 66, no. 5, pp. 3622–3631, May 2017.
- [15] O. Erdinc, N. G. Paterakis, T. D. P. Mendes, A. G. Bakirtzis, and J. P. S. Catalão, "Smart household operation considering bi-directional EV and ESS utilization by real-time pricing-based DR," *IEEE Trans. Smart Grid*, vol. 6, no. 3, pp. 1281–1291, May 2015.
- [16] M. H. K. Tushar, A. W. Zeineddine, and C. Assi, "Demand-side management by regulating charging and discharging of the EV, ESS, and utilizing renewable energy," *IEEE Trans. Ind. Inform.*, vol. 14, no. 1, pp. 117–126, Jan. 2018.

- [17] H. Turker and S. Bacha, "Optimal minimization of plug-in electric vehicle charging cost with vehicle-to-home and vehicle-to-grid concepts," *IEEE Trans. Veh. Technol.*, vol. 67, no. 11, pp. 10281–10292, Nov. 2018.
- [18] S. Merrington, R. Khezri, and A. Mahmoudi, "Optimal planning of solar photovoltaic and battery storage for electric vehicle owner households with time-of-use tariff," *IET Gener., Transmiss., Distrib.*, vol. 16, no. 3, pp. 535–547, Feb. 2022.
- [19] R. Khezri, A. Mahmoudi, and M. H. Haque, "Impact of optimal sizing of wind turbine and battery energy storage for a grid-connected household with/without an electric vehicle," *IEEE Trans. Ind. Inform.*, vol. 18, no. 9, pp. 5838–5848, Sep. 2022.
- [20] H. Hua, Y. Qin, C. Hao, and J. Cao, "Optimal energy management strategies for energy Internet via deep reinforcement learning approach," *Appl. Energy*, vol. 239, pp. 598–609, Apr. 2019.
- [21] S. Hasavand, M. Rafiei, M. Gheisarnejad, and M. Khooban, "Reliable power scheduling of an emission-free ship: Multiobjective deep reinforcement learning," *IEEE Trans. Transp. Electric.*, vol. 6, no. 2, pp. 832–843, Jun. 2020.
- [22] M. Electric, "What is the difference between slow, fast and rapid EV chargers?", Aug. 2022. Accessed: Oct. 25, 2022. [Online]. Available: <https://www.motoringelectric.com/charging/difference-between-slow-fast-rapid-charging/>
- [23] N. A. Orlando, M. Liserre, R. A. Mastromauro, and A. Dell'Aquila, "A survey of control issues in PMSG-based small wind-turbine systems," *IEEE Trans. Ind. Inform.*, vol. 9, no. 3, pp. 1211–1221, Aug. 2013.
- [24] 2017 Small Wind World Report Summary, Jun. 2017. Accessed: Sep. 25, 2022. [Online]. Available: [http://www.wwindea.org/download/SWWR2017-SUMMARY\(2\).pdf](http://www.wwindea.org/download/SWWR2017-SUMMARY(2).pdf)
- [25] R. Khezri, A. Mahmoudi, and M. H. Haque, "A demand side management approach for optimal sizing of standalone renewable-battery systems," *IEEE Trans. Sustain. Energy*, vol. 12, no. 4, pp. 2184–2194, Oct. 2021.
- [26] E. E. Elattar, J. Y. Goulermas, and Q. H. Wu, "Generalized locally weighted GMDH for short term load forecasting," *IEEE Trans. Syst., Man, Cybern.*, vol. 42, no. 3, pp. 345–356, May 2012.
- [27] M. Loureiro, P. Agamez-Arias, T. J. A. Abreu, and V. Miranda, "A DEEPSO-GMDH model for supporting the battery energy storage investment planning decision-making," in *Proc. 6th IEEE Int. Energy Conf.*, 2020, pp. 539–544.
- [28] H. R. Madala and O. G. Ivakhnenko, *Inductive Learning Algorithms for Complex Systems Modeling*. Boca Raton, FL, USA: CRC Press, 1994.
- [29] Australian Government, Bureau of Meteorology. Climate Data Online, Accessed: Sep. 2021. [Online]. Available: <http://www.bom.gov.au/climate/data/index.shtml?bookmark=200>
- [30] SA Power Networks Limits Three-Phase Exports To 15kW, Jun. 2019. Accessed: Sep. 25, 2021. [Online]. Available: <https://www.solarquotes.com.au/blog/sa-three-phase-solar/>
- [31] Residential Charging Stations, Accessed: Sep. 25, 2021. [Online]. Available: <https://evse.com.au/home-ev-charging/>
- [32] H. Ren, Z. Ma, W. Lin, S. Wang, and W. Li, "Optimal design and size of a desiccant cooling system with onsite energy generation and thermal storage using a multilayer perceptron neural network and a genetic algorithm," *Energy Convers. Manage.*, vol. 180, pp. 598–608, 2019.
- [33] Z. Hou, J. Guo, J. Xing, C. Guo, and Y. Zhang, "Machine learning and whale optimization algorithm based design of energy management strategy for plug-in hybrid electric vehicle," *IET Intell. Transport Syst.*, vol. 15, no. 8, pp. 1076–1091, 2021.



**Rahmat Khezri** (Member, IEEE) received the M.S. degree in electrical engineering from the University of Kurdistan, Sanandaj, Iran, in 2014, and the Ph.D. degree in electrical engineering from Flinders University, Adelaide, SA, Australia, in 2021. From November 2019 to October 2020, he was a Research Fellow with the University of Tsukuba, Tsukuba, Japan. From January to June 2021, he was a Visiting Scholar with Aarhus University, Aarhus, Denmark. He is currently a Postdoctoral Researcher with the Chalmers University of Technology, Gothenburg, Sweden. His research interests include power system planning and operation, energy management, electric vehicle, and energy storage system.



**Peyman Razmi** received the M.Sc. degree in electrical engineering from the Ferdowsi University of Mashhad, Mashhad, Iran, in 2015. He is currently with the IPB, Portuguese Institute and the University of Porto Porto, Portugal, as a Research Fellow Member. His main research interests include electricity market, machine learning, convex and stochastic optimization, and application of game theory in the deregulated power market.



**Amin Mahmoudi** (Senior Member, IEEE) received the B.Sc. degree in electrical engineering from Shiraz University, Shiraz, Iran, in 2005, the M.Sc. degree in electrical power engineering from the Amirkabir University of Technology, Tehran, Iran, in 2008, and the Ph.D. degree in electrical engineering from the University of Malaya, Kuala Lumpur, Malaysia, in 2013.

He is currently a Lecturer with Flinders University, Adelaide, SA, Australia. He has authored or coauthored more than 150 papers in international journals and conferences. His main research interests include areas where the electrical energy conversion plays a major role, such as the electrical machines and drives and the renewable energy systems and hybrid power networks. It includes the transportation electrification in which the sustainable energy efficient solutions are realized by advanced electric motors, power electronics, energy management systems and controls for electrified powertrains, and electric vehicles.

Dr. Mahmoudi is a Member of the Institution of Engineering and Technology and a Chartered Engineer. He is also a Member of the Engineers Australia and a Chartered Professional Engineer.



**Ali Bidram** (Senior Member, IEEE) received the B.Sc. and M.Sc. degree from the Isfahan University of Technology, Isfahan, Iran, in 2008 and 2010, respectively, and the Ph.D. degree from the University of Texas at Arlington, Arlington, TX, USA, in 2014. He is currently an Assistant Professor with the Electrical and Computer Engineering Department, the University of New Mexico, Albuquerque, NM, USA. Before joining the University of New Mexico, he was with Quanta Technology, LLC, and was involved in a wide range of projects in the electric power industry.

His area of expertise lies within the control and protection of energy assets in power electronics-intensive energy distribution grids. Such research efforts culminated in a book, several journal papers in top publication venues and articles in peer-reviewed conference proceedings, and technical reports. He was the recipient of the University of New Mexico's School of Engineering junior faculty teaching excellence Award, IEEE Albuquerque section outstanding engineering educator Award, New Mexico EPSCoR mentorship Award, University of Texas at Arlington N. M. Stelmakh outstanding student research Award, IEEE Kansas Power and Energy Conference Best Paper Award, and cover article of December 2014 in IEEE Control Systems.



**Mohammad Hassan Khooban** (Senior Member, IEEE) received the Ph.D. degree in power systems and electronics from the Shiraz University of Technology, Shiraz, Iran, in 2017. From 2016 to 2017, he was a Research Assistant with Aalborg University, Aalborg, Denmark, where he conducted research on advanced control of microgrids and marine power systems. From 2017 to 2018, he was a Postdoctoral Associate with Aalborg University. From 2019 to 2020, he was a Postdoctoral Research Assistant with Aarhus University, Aarhus, Denmark, where he is currently an Assistant Professor. He is also the Director of the Power Circuits and Systems Laboratory. He has authored or coauthored more than 240 publications on journals and international conferences, three book chapters, and holds one patent.

His research interests include control theory and application, power electronics, and its applications in power systems, industrial electronics, and renewable energy systems.